Casimir interactions between graphene sheets and metamaterials

D. Drosdoff and Lilia M. Woods

Phys. Rev. A **84**, 062501 — Published 2 December 2011

DOI: 10.1103/PhysRevA.84.062501

Casimir Interactions between Graphene Sheets and Metamaterials

D. Drosdoff and Lilia M. Woods

Department of Physics, University of South Florida, Tampa FL 33620

Abstract

The Casimir force between graphene sheets and metamaterials is studied. Theoretical results based on the Lifshitz theory for layered, planar, two dimensional systems in media are presented. We consider graphene/graphene, graphene/metamaterial, and metal/graphene/metamaterial configurations. We find that quantum effects of the temperature dependent force are not apparent until the sub-micron range. In contrast to results with bulk dielectric and bulk metallic materials, no Casimir repulsion is found when graphene is placed on top of a magnetically active metamaterial substrate, regardless of the strength of the low frequency magnetic response. In the case of the metal/graphene/metamaterial setting, repulsion between the metamaterial and the metal/graphene system is possible only when the dielectric response from the metal contributes significantly.

PACS numbers: 42.50.LC,78.67.Wj,78.67.Pt

I. INTRODUCTION

As the length scale of electronic devices decreases, electromagnetic fluctuation forces, such as Casimir forces, become increasingly important. To a large extent this is due to unwanted effects from stiction, friction, or adhesion in various nanostructured systems[1, 2]. Finding ways of reducing these fluctuation forces, therefore, has important applications to the manufacturing of miniaturized devices.

The Casimir force is a fundamental interaction present at all length scales. Such a force is strongly dependent on the distance separating the interacting objects, their geometry, and the type of materials[3, 4]. In most situations the Casimir force is attractive. However, recently the possibility of reducing the magnitude of the attraction or even obtaining a Casimir repulsion has gained much interest. One possibility of obtaining repulsion, described theoretically[5] and demonstrated experimentally[6], involves ordering planar structures with dielectric functions in a specific way - given three stacked dielectric materials with $\epsilon_1 > \epsilon_2 > \epsilon_3$ or $\epsilon_1 < \epsilon_2 < \epsilon_3$, where ϵ_i is the dielectric permittivity for each medium.

A repulsive Casimir force can also be obtained when a mostly dielectric material interacts with a mostly magnetic one[7–9]. This effect is strongest in the micron range if the materials can sustain relatively strong magnetic response in the optical or infrared regimes. Since no naturally occurring materials have significant permeabilities for optical frequencies, metamaterials (MMs) have become a candidate for obtaining Casimir repulsion[7, 9, 10]. Usually, MMs are fabricated by making a composite with building blocks smaller than the wavelength of the incoming radiation within some medium, which allows for obtaining a significant magnetic response in the infrared and optical frequency regime[11].

Unfortunately, stability due to Casimir forces cannot be obtained from metamaterials which arise from a combination of regular dielectrics and metals alone[3]. Instead Casimir repulsive forces have been investigated with metamaterials containing magnetically active components, such as superparamagnetic nanoparticles embedded in a dielectric medium [13, 14]. It has been found that Casimir repulsion between these superparamagnetic metamaterials and other materials is possible.

The recent isolation of graphene[15, 16] from graphite has led to a spurt of research aimed to understand its fundamental properties. In addition, graphene has become a promising material for the development of high frequency transistors[17], biological sensors[18]

and ultra-capacitors[19]. The Casimir force between graphene layers was recently studied theoretically[20, 37, 39], and it was demonstrated that due to its two dimensional nature and dielectric transparency the force can be significantly reduced compared to perfect metallic systems. It is interesting to pursue further interactions between graphene sheets as well as graphene and other materials, especially MMs, to uncover new functionalities. In this work, we investigate the Casimir force in graphene/graphene, graphene and metallic/dielectric based MMs, and graphene and superparamagnetic MMs (SP-MMs) systems, including its dielectric and magnetic properties, as well as its temperature effects.

The paper is organized as follows. In Sec.II, the generalized Lifshitz expression for the Casimir interaction in a planar system is reviewed. In Sec.III, models for the electrical and magnetic properties of graphene and MMs are given. In Sec.IV the force between graphene sheets is studied. In particular, the work on graphene is extended to include the effects of the higher frequency interband transition modes and the relative importance of temperature to the force. In Sec.V, the Casimir forces between graphene and magnetically active metamaterials are studied. Conclusions follow in Sec.VI.

II. LIFSHITZ CASIMIR FORMULA

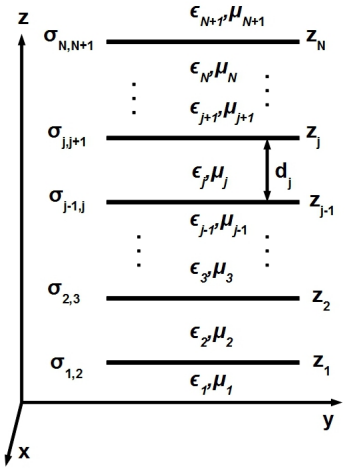

FIG. 1. N infinitely thin sheets sandwiched in $N+1$ media layers and separated by distances $d_j = z_j - z_{j-1}$. The sheets extend in the $x-y$ plane. Their conductivities and positions along the z-axis are shown. The dielectric and magnetic functions of the media between the graphene sheets are denoted as ϵ_j and μ_j, respectively.

We consider the Casimir interaction between two adjacent, parallel, infinitely thin sheets in a composite of N such sheets immersed in media - Fig.(1). Each sheet is characterized by an isotropic two dimensional conductivity $\sigma_{j,j+1}$ and the layers of thickness d_j are filled with media with dielectric $\epsilon_j(\omega)$ and magnetic $\mu_j(\omega)$ functions. The Casimir force per unit area in layer j at finite temperature[29] is given by

$$F_j = -\frac{ik_BT}{2\pi}\sum_{n=-\infty}^{\infty}\int_0^{\infty} h_j(i|\omega_n|)k_\perp dk_\perp \left\{\left[\frac{e^{-2ih_j(i|\omega_n|)d_j}}{\rho_{Ej}^{+}(i|\omega_n|)\rho_{Ej}^{-}(i|\omega_n|)}-1\right]^{-1}+\left[\frac{e^{-2ih_j(i|\omega_n|)d_j}}{\rho_{Bj}^{+}(i|\omega_n|)\rho_{Bj}^{-}(i|\omega_n|)}-1\right]^{-1}\right\}, \tag{1}$$

where $h_j(i|\omega_n|) = i\sqrt{\epsilon_j(i|\omega_n|)\mu_j(i|\omega_n|)(\omega_n/c)^2 + k_\perp^2}$ with $\omega_n = 2\pi n k_B T/\hbar$ and $k_\perp$ - the two-dimensional wave vector in the xy-plane. Also, T is the temperature, d_j is the separation between the two adjacent sheets, k_B is Boltzmann constant, and $\rho_{Ej,Bj}^{\pm}$ are the generalized reflection coefficients due to the transverse electric ($\mathbf{E}$) and magnetic ($\mathbf{B}$) field modes from the top ($+$) and the bottom ($-$) of layer j.

We calculate the interaction between two graphene sheets, graphene and half-space substrate, and graphene sandwiched between two half-space materials. All configurations are in vacuo. The reflection coefficients in each case can be found via an iterative procedure described in[30]. In the case of two graphene sheets in a vacuum, we obtain

$$\begin{aligned}\rho_E^{+} &= \rho_E^{-} = -\frac{2\pi\omega\sigma/(hc^2)}{1+2\pi\omega\sigma/(hc^2)},\\ \rho_B^{+} &= \rho_B^{-} = \frac{2\pi\sigma h/\omega}{1+2\pi\sigma h/\omega},\end{aligned} \tag{2}$$

where $(+)$ defines the top and $(-)$ the bottom sheet. Also, $h = i\sqrt{\omega_n^2/c^2 + k_\perp^2}$ and σ is the conductivity of graphene.

In the case of graphene above a substrate, the coefficients are given by

$$\rho_E^{-} = \frac{\mu_1 h - h_1}{\mu_1 h + h_1}, \quad \rho_B^{-} = \frac{\epsilon_1 h - h_1}{\epsilon_1 h + h_1}, \tag{3}$$

where μ_1 (magnetic permeability), ϵ_1 (dielectric function) and $h_1 = i\sqrt{\epsilon_1(i|\omega_n|)\mu_1(i|\omega_n|)(\omega_n/c)^2 + k_\perp^2}$ refer to the substrate. $\rho_{E,B}^{+}$ are the same as in Eq.(2)

Finally, for graphene between two semi-infinite substrates, the reflection coefficients in

the layer between graphene and the bottom substrate (layer 2 - Fig.(1)) are

$$\rho^{+}_{E2} = \frac{(h+h_4)\rho^{+}_{E} + (1+2\rho^{+}_{E})(h-h_4)e^{2ih_3d_3}}{(h+h_4) - \rho^{+}_{E}(h-h_4)e^{2ih_3d_3}},$$
$$\rho^{+}_{B2} = \frac{(h_4+\epsilon_4 h)\rho^{+}_{B} + (1-2\rho^{+}_{B})(\epsilon_4 h-h_4)e^{2ih_3d_3}}{(h_4+\epsilon_4 h) - \rho_{B}(\epsilon_4 h-h_4)e^{2ih_3d_3}} \tag{4}$$

where $h_4 = i\sqrt{\epsilon_4(i|\omega_n|)\mu_4(i|\omega_n|)\omega_n^2/c^2 + k_\perp^2}$ and $\rho^{-}_{E2,B2}$ are given by Eq.(3).

III. RESPONSE PROPERTIES OF GRAPHENE AND METAMATERIALS

The substrates of interest here are comprised of metamaterials and metals. We describe the relevant models for the response properties of each type of material, since the dielectric and magnetic functions, and the sheet conductivities are necessary to calculate the Casimir force - Eq.(1).

The response properties of the metallic materials are given via the usual Drude model,

$$\epsilon_M(\omega) = 1 - \frac{\Omega_M^2}{\omega^2 + i\gamma_M\omega}, \quad \mu_M(\omega) = 1, \tag{5}$$

where Ω_M is the plasma frequency strength and γ_M is the dissipation frequency.

The low frequency optical conductivity of graphene is calculated using a two-band Dirac model for the energy bandstructure[23, 38],

$$\sigma(\omega) = \sigma_{intra}(\omega) + \sigma_{inter}(\omega)$$
$$\sigma_{intra}(\omega) = -\frac{2ie^2}{\hbar^2\pi(\omega+i\Gamma)}\int_0^\infty dE E\frac{df_0(E)}{dE} = \frac{2ie^2k_BT\ln(2)}{\pi\hbar^2(\omega+i\Gamma)}$$
$$\sigma_{inter}(\omega) = \frac{ie^2(\omega+i\Gamma)}{\pi}\int dE\frac{f(-E)-f(E)}{\hbar^2(\omega+i\Gamma)^2+4E^2}, \tag{6}$$

where σ_{intra} is the conductivity due the intraband and σ_{inter} is the conductivity due to the interband transitions. Γ is the scattering rate and $f_0(E) = 1/[\exp(E/k_BT)+1]$ with E being the energy.

In the infrared and low optical frequency regime ($< 3\ eV$) and low T, when $k_BT < \hbar\omega$ and $\Gamma \approx 0$[38], the graphene conductivity is constant with a universal value $\sigma_0 = e^2/4\hbar$. This has also been shown experimentally[22]. For higher frequencies, *ab initio* calculations reveal that the optical response properties of in-plane graphite and graphene are very similar[24, 25]. The in-plane graphite dielectric response has also been mapped into a sum of Lorentz-type harmonic oscillators[26]. To account for these findings, here the conductivity of a single

graphene layer, $\sigma(\omega)$, is described by Eq.(6) for $\hbar\omega \leq 3\ eV$ and by the Lorentz sum model for the higher energies. The dispersion, which becomes important at shorter distances will not be taken into account.

Metamaterials are artificially fabricated structures made out of dielectric and/or metallic components, in which one can achieve a negative index of refraction over a certain range of frequencies[40]. Exotic properties, such as substantial magnetic response in the infrared and low optical regime, negative permittivity and negative permeability have been observed[41–48]. Partially metallic MMs have been fabricated to demonstrate these phenomena. In particular, split ring resonators are found to operate in the GHz-THz range, and fishnet structures are suitable for the near-infrared-optical range[44]. The dielectric response of such a MM can be modeled using a one oscillator Lorentz-like isotropic model with the contribution from the metallic connected environment taken into account via a Drude term[10]

$$\epsilon(\omega) = 1 - \frac{(1-f)\Omega_e^2}{\omega^2 - \omega_e^2 + i\omega\gamma_e} - \frac{f\Omega_D^2}{\omega^2 + i\omega\gamma_D}, \tag{7}$$

where Ω_e is the electric response plasma frequency for the dielectric component of the metamaterial, ω_e is the resonance frequency, and γ_e is the dissipation frequency term. The metallic component plasma frequency is given by Ω_D, and the dissipation term - by γ_D. The filling factor f accounts for the fraction of metallic structures present in the MM. By varying f, one can use different quantities of metallic structures and tune the dielectric response of the MM.

The modeling of the MM magnetic response is an important issue for the calculation of the Casimir interaction. Since most of the magnetic activity is in the low frequency regime, using the effective medium approach for larger distances, Pendry[12] derived

$$\mu_P(\omega) = 1 - p\frac{\omega^2}{\omega^2 - \omega_m^2 + i\gamma_m\omega}, \tag{8}$$

where p is a filling factor (p is always between 0 and 1), ω_m is the magnetic resonance location, and γ_m is the dissipation frequency. A peculiar feature here is the presence of ω^2 in the numerator of Eq.(8).

MMs made from superparamagnetic nanospheres immersed in some weak dielectric medium have also become of interest due to their substantial magnetic response in the low optical regime. Such composites can be constructed from ferromagnetic metallic nanostructures with large saturation magnetization, such as Ni or Fe, immersed in a matrix of

Al_2O_3[13] or polystyrene[14]. Here we consider superparamagnetic MMs composed of Ni or Fe nanoparticles in polystyrene for the graphene/SP-MM interaction. The dielectric properties of such a porous composite is given by the Maxwell-Garnett equation derived from an effective medium approach[28],

$$\frac{\epsilon_{SP} - \epsilon_0}{\epsilon_{SP} + 2\epsilon_0} = \sum_{i=1}^{n} f_i \frac{\epsilon_i - \epsilon_0}{\epsilon_i + 2\epsilon_0}, \tag{9}$$

where ϵ_{SP} is the effective permittivity of the material, ϵ_0 is the dielectric constant of the medium, and ϵ_i is the permittivity of the components embedded in the medium, while f_i is the volume fraction of each component. For the composite here, we have two components - polystyrene with f_p, ϵ_p and metallic spheres with f_M, ϵ_M. ϵ_p is modeled as a sum of four harmonic oscillators[29], while ϵ_M is described via a plasma model($\gamma_M = 0$) with plasma frequencies for Ni and Fe - $\Omega_{Ni} = 3.94\ eV$ and $\Omega_{Fe} = 15\ eV$[31]. The medium is taken to be air(vacuum).

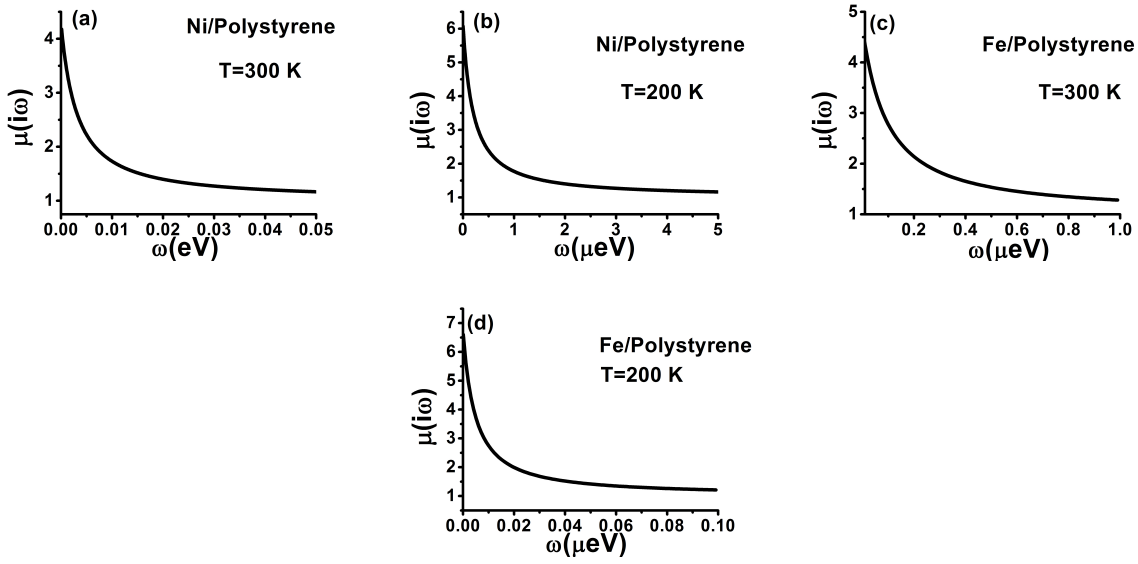

FIG. 2. $\mu(i\omega)$ as a function of ω for Ni nanospheres in polystyrene at (a) T=300 K with $K = 5 \times 10^4\ erg/cm^3$ (b) T=200 K with $K = 3 \times 10^5\ erg/cm^3$. Other parameters are $a = 5\ nm$, $m_0 = 480\ Gauss$, and $f_1 = 0.2$. $\mu(i\omega)$ as a function of ω for Fe nanospheres in polystyrene at (c) T=300 K; (d) T=200 K with parameters $K = 8.8 \times 10^6\ erg/cm^3$, $a = 1.9\ nm$, $m_0 = 1800\ Gauss$, and $f_1 = 0.29$.

The permeability of the composite on the other hand is modeled by an extended Onsager

formula[32]. In the limit of small particle size[14] one obtains

$$\mu_{SP}(\omega) = \frac{1}{4}\left[1 + \frac{4\pi R f_1}{1 - i\omega\tau} + \sqrt{8 + \left(1 + \frac{4\pi R f_1}{1 - i\omega\tau}\right)^2}\right], \tag{10}$$

where f_1 is the fraction of the nanoparticles, $R = \frac{4\pi a^3 m_0^2}{3k_B T}$ with a being the nanoparticle radius and m_0 - the saturation magnetization. For dilute samples, the magnetization relaxation time τ has been shown to follow the Arrhenius law[33] given by

$$\tau = \tau_0 e^{KV/(k_B T)}, \tag{11}$$

where K is the magnetic anisotropic energy, $V = 4\pi a^3/3$ is the particle volume and $\tau_0 \approx 10^{-13}$ s[34]. If the concentration of metallic nanoparticles increases, other interactions such as dipolar couplings[35] affect τ and Eq.(11) has to be modified. Here we assume that the Arrhenius law is valid and no modifications are necessary.

The permeability of the superparamagnetic material depends strongly on practically all characteristics entering Eq.(10). Here we calculate it at two different temperatures as a function of frequency. Results from Fig.(2) show that significant magnetic response lies in the infrared regime for both types of SP-MMs.

IV. CASIMIR FORCES BETWEEN GRAPHENE SHEETS

The magnitude of the Casimir force per unit area between two graphene sheets (F) separated by a distance d is calculated using Eq.(1). At zero temperature, it has been found that the stress F between graphene sheets is attractive, and it is inversely proportional to d^4[36, 37], as in the case of two perfect metallic plates, but with a much smaller coefficient. Interestingly it does not depend on Plank's constant $\hbar$ or the speed of light c - $F = 3e^2/(32\pi d^4)$[20].

For finite temperatures, the Casimir interaction is determined by a characteristic length, which in regular 3-D bulk materials is $\lambda_T = \hbar c/(k_B T)$. However, due to the two dimensional nature of graphene and its unique linear $k_\perp$ dependence in its low energy dispersion, the characteristic length is found to be $\xi_T \sim 2.5\hbar\sigma/(k_B T) \approx \lambda_T/200$. At room temperature, for example, $\xi_T \approx 25$ nm, which is greatly reduced from $\lambda_T \approx 5\mu m$ for systems made of bulk materials. At distances $d > \xi_T$, the force per unit area is dominated[37] by the first

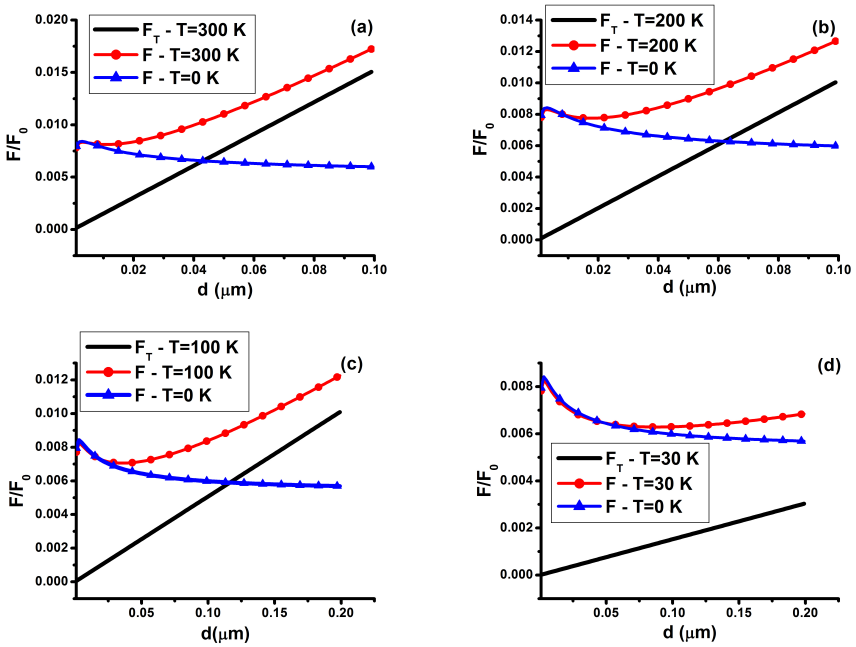

FIG. 3. (Color Online) Casimir force normalized to the force between two perfect metallic plates between two graphene sheets as a function of their separation d calculated using the full Matsubara sum, the 0th term (F_T) and the zero temperature limit integral expression at a) T=300 K; b) T=200 K; c) T=100 K; d) T=30 K.

term(n=0) of Eq.(1),

$$F_T = \frac{k_B T \zeta(3)}{8\pi d^3}, \tag{12}$$

where $\zeta(3) = 1.202$. On the other hand, the dielectric properties beyond the two-band model[24, 25] imply that graphene would have a strong dielectric response at higher frequencies, resulting in ξ_T becoming larger. Therefore more terms from the Matsubara sum in Eq.(1) would be needed at larger distances. We point out that when $d \ll \xi_T$, terms with larger n are dominant and the ω_n sum in Eq.(1) can be turned into an integral over ω. Such integral representation is exact at $T = 0\ K$. Using the graphene response given as a sum of Lorentz oscillators [26], the Casimir force per area between two graphene sheets normalized to the force per area between two perfect metallic plates(F_0) is given in Fig.(3). The interaction(F) calculated using Eq.(1) and Eq.(12) is shown at different temperatures. The stress at $T = 0\ K$ is obtained via the integral representation of Eq.(1).

Fig.(3) shows that for larger temperatures and smaller distances ($d < 100\ nm$ for $T =$

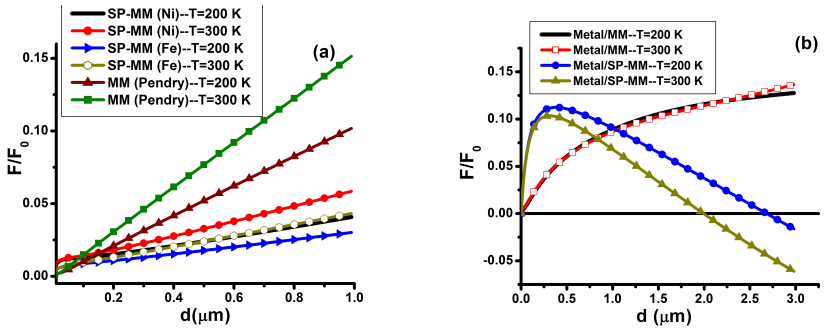

FIG. 4. (Color Online) (a) Casimir stress between graphene and a MM substrate as a function of distance d at $T = 200K$, $T = 300K$. (b) Casimir stress between a metallic and a MM substrates as a function of distance d at $T = 200$ and $T = 300K$. F_0 is the stress between two ideal metals, while the plasma frequency of the metal is $\Omega_M = 10\ eV$ and $\gamma_M = 0$.

$100\ K$ and $d < 40\ nm$ for $T = 300\ K$, for example), the force per unit area is described by its full expression Eq.(1). For larger distances, the interaction is essentially given by the F_T expression, which corresponds to the force due to classical thermal fluctuations, i.e., the $n = 0$ term in the Matsubara sum of Eq.(1)[27]. At smaller temperatures, Fig.(3(d)), F_T is a poor approximation for increasingly larger distances, and there is little difference between the stress obtained via Eq.(1) and the integral representation at the $T = 0\ K$ limit.

V. CASIMIR FORCES IN GRAPHENE/METAMATERIAL SYSTEMS

Here we consider the interaction between graphene and a MM substrate in a vacuum. Using Eqs.(1,2,3), the calculated stress is presented in Fig.(4(a)) for metallic based MMs with response properties described in Eqs.(7,8) and for superparamagnetic MMs(SP-MM) with response properties from Eqs.(9,10). In all cases, the force is always attractive. The characteristic behavior for the magnetically active MM and the Pendry model type MM is similar. It is seen that the temperature affects the Casimir interaction significantly. We find that at relatively high temperatures the dominant contribution comes from the $n = 0$ term of Eq.(1). It also appears that the filling factor has little effect on the interaction, since different values of p gave very similar results for F. For the SP-MM, in addition to the T dependence in the expression for the stress, the T dependence of R and τ in the permeability have significant contributions, as this changes the form of the attraction, clearly noted at

shorter distances.

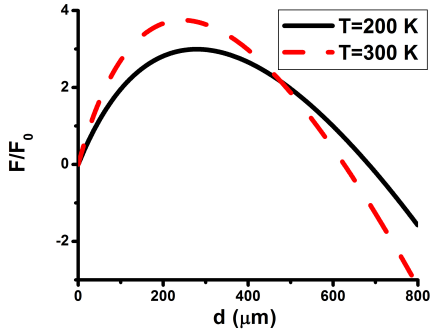

FIG. 5. (Color Online) Casimir force normalized to the one for ideal metallic plates between pure graphene and SP-MM (Ni nanoparticles) as a function of their separation d at $T = 200K$ and $T = 300K$.

We also compare the graphene/MM interaction with the one in a metal/MM system - Fig.(4(b)). The force per unit area between the metallic half space and the Pendry model MM half space (μ_P) is again always attractive. However, when there is a superparamagnetic MM, F changes sign at a certain distance and the interaction becomes repulsive. This is similar to previously obtained results, where Casimir repulsion has been found in systems with materials exhibiting superparamagnetism[13, 14]. The repulsion is due to the large magnetic response of the metamaterial at low frequencies.

The reason for the lack of repulsion in the graphene/SP-MM lies in the form of the reflection coefficients, Eq.(2). Using σ from Eq.(6), one finds that $\rho_E^- \rho_E^+ = 0$ and $\rho_B^- \rho_B^+ = \rho_B^-$ for $n = 0$, the zero frequency limit. This implies that the transverse magnetic component of the reflection coefficients determines the force, and the magnetic response from the superparamagnet does not contribute significantly. Consequently, no repulsion is possible at larger temperatures in the graphene/SP-MM system. In order to obtain a repulsion, a significant contribution from the transverse electric component - ρ_E^+ - from the two dimensional material is necessary. This can be achieved if the two dimensional material has a response at low frequencies going as $\sigma(\omega) \sim 1/\omega$. In the case of graphene, this is possible if one sets $\Gamma = 0$ in Eq.(6), which corresponds to a very pure system with no defects. In this case, at low frequencies and high temperatures, $\hbar\omega \ll k_B T$, the conductivity (Eq.(6)) is found to be [38]

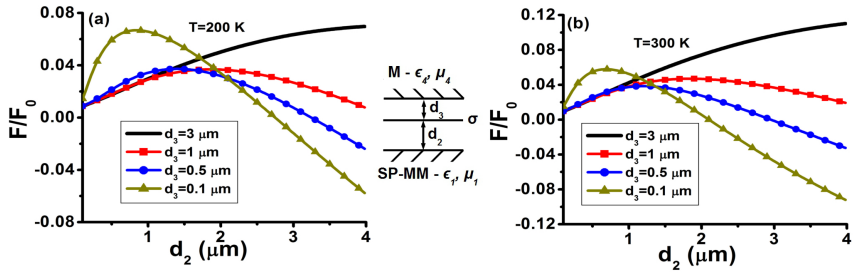

FIG. 6. (Color Online) Casimir force per unit area between the metal/graphene system and the MM as a function of the separation d_2 for several metal/graphene distances d_3 at (a) $T = 200$ K; (b) $T = 300$ K. F_0 is the force per unit area between two ideal metallic plates. The insert depicts the system under consideration composed of metallic substrate/graphene/MM substrate.

$$\sigma(i\omega) = 2\ln 2\frac{e^2 k_B T}{\pi\hbar^2\omega} + \frac{\sigma_0\hbar\omega}{2\pi k_B T}\ln\left(\frac{k_B T}{\hbar\omega}\right). \tag{13}$$

Therefore $\rho_E^- \rho_E^+ \neq 0$, which can allow for a repulsive force at some finite distance due to the low frequency magnetic response of the SP-MM. Fig.(5) shows the stress between graphene, described via Eq.(13), and a superparamagnetic composite. There is indeed a distance in which the force becomes repulsive, but this distance is extremely large (close to 1 mm) in the context of Casimir forces.

Further we study the interaction of a system composed of graphene sandwiched between a MM and a metallic substrate, as shown in the insert of Fig.(6). The presence of the metal on top of the graphene reduces the distance at which repulsion may be exhibited. For different metal/graphene separations d_3, F/F_0 is given as a function of the distance, d_2, between the graphene and the MM. The stress is essentially calculated as an effective interaction between the materials below (MM) and above (graphene and metal system) the layer using Eqs.(3,4). Results are shown for the Ni nanoparticles in polystyrene at two temperatures - Figs.(6(a),6(b)). It is seen that for larger graphene/metal separations, the stress is attractive in the shown d_2 range. For smaller d_3 separations, however, F/F_0 is characterized with a maximum, and for a certain distance d_2, the force changes sign and becomes repulsive.

These results can be understood by realizing that when the graphene and metal are far apart from each other, the MM will 'see' the materials above it as mostly graphene-like, and the contribution from the metal is relatively small. The Casimir interaction is always

attractive in this case, since the force per area between the two-component SP-MM/graphene is always attractive. When the graphene and metal are relatively close, the most significant contribution of the response comes from the metal. Thus the stress exhibits a repulsive region as obtained for the metal/SP-MM system - Fig.(6).

VI. CONCLUSION

The Casimir force between graphene sheets and between graphene and metamaterials were studied. It was shown that, at higher temperatures, the stress between graphene sheets is essentially classical in the micron scale, yet at scales smaller than 0.05 μm, quantum effects become important from the larger oscillator frequency modes in graphene. These quantum effects become more pronounced and with a longer range as the temperature is lowered such that by $T = 30K$ quantum mechanical effects are substantial close to the micron range.

Two types of metamaterials were considered. One is a composite made out of regular dielectrics and metals; the other is a magnetically active metamaterial constructed from superparamagnetic nanostructures. We find that the Casimir interaction is always attractive in the micrometer range for the graphene/MM system for both MM types. This is unlike the case of a metal/superparamagnetic MM system. The magnetic properties of the SP-MM do not strongly interact with two dimensional graphitic systems, because of the particular form of the reflection coefficients and the graphene response properties. Only at very large distances it could be possible to obtain repulsion, given a Drude response of graphene at very low frequencies and very large transport scattering time. Metal/graphene/MM systems were also considered and explained in terms of the relative contribution from the response properties of the metal and graphene components to the effective interaction.

Casimir forces in graphene systems highlight the differences between two dimensional structures and three dimensional bulk ones, as well as particularities in the response properties of graphene as compared to regular materials. The reduced range of the quantum mechanical effects on the fluctuations forces is particularly interesting. As a next step it would be important to consider further the effects from a change in the chemical potential[49] on the graphitic layers as well as the inclusion of the full dispersion in their dielectric response.

VII. ACKNOWLEDGEMENTS

We acknowledge financial support from the Department of Energy under contract DE-FG02-06ER46297.

---

[1] H. B. Chan, V. A. Aksyuk, R. N. Kleiman, D. J. Bishop, and F. Capasso, *Phys. Rev. Lett.* **87**, 211801 (2001).

[2] H. B. Chan, et. al., *Science* **291**, 1941 (2001).

[3] S. J. Rahi, M. Kardar, and T. Emig, *Phys. Rev. Lett.* **105**, 070404 (2010).

[4] M. Bordag, U. Mohideen, and V. M. Mostepanenko, *Phys. Rep.* **353**, 1 (2001); K. Milton, *J. Phys. A* **37**, R209 (2004).

[5] I. E. Dzyaloshinskii, E. M. Lifshitz, and L. P. Pitaevskii, *Adv. Phys.* **10**, 165 (1961).

[6] J. N. Munday, F. Capasso, and A. Parsegian, *Nature* **457**, 170 (2009).

[7] T. H. Boyer, *Phys. Rev. A* **9**, 2078 (1974).

[8] O. Kenneth, I. Klich, A. Mann, and M. Revzen, *Phys. Revv Lett.* **89**, 033001 (2002).

[9] I. G. Pirozhenko and A. Lambrecht, *J. Phys. A:Math. Theor.* **41**, 164015 (2008).

[10] F. S. S. Rosa, D. A. .R. Dalvit, and P. W. Milonni, *Phys. Rev. A* **78**, 032117 (2008); F. S. S. Rosa, D. A. R. Dalvit, and P. W. Milonni, *Phys. Rev. Lett.* **100**, 183602 (2008).

[11] R. Marqués, F. Martín and M. Sorolla, *Metamaterials with Negative Parameters*, John Wiley & Sons Inc., Hoboken (2008).

[12] J. B. Pendry, A. J. Holden, D. J. Robbins, W. J. Stewart, *IEEE Trans. Microwave Theory Tech.* **47**, 2075 (1999).

[13] V. Yannopapas and N. V. Vitanov, *Phys. Rev. Lett.* **103**, 120401 (2009).

[14] Norio Inui, *Phys. Rev. A* **83**, 032513 (2011).

[15] K. S. Novoselov, A. K. Geim, S. V. Morozov, D. Jiang, Y. Zhang, S. V. Dubonos, I. V. Grigorieva, and A. A. Firsov, *Science* **360**, 666 (2004).

[16] K. S. Novoselov, D. Jiang, F. Schedin, T. J. Booth, V. V. Khotkevich, S. V. Morozov, and A. K. Geim, *Proc. Nat. Acd. Sci.* **102**, 10451 (2005).

[17] Y. M. Lin, C. Dimitrakopoulos, K. A. Jenkins, D. B. Farmer, and H. Y. Chiu, *Science* **327**, 662 (2010).

[18] Y. Shao, J. Wang, H. Wu, J. Liu, I. A. Aksay, Y. Lin, *Electroanalysis* **22**, 1027 (2010).

[19] M. D. Stoller, S. Park, Y. Zhu, J. An, and R. S. Ruoff, *Nano Letters* **8**, 3498 (2008).

[20] D. Drosdoff and L. M. Woods, *Phys. Rev. B* **82**, 155459 (2010).

[21] E. M. Lifshitz, *J. Exper. Theoret. Phys. USSR* **29**, 94 (1955).

[22] R. R. Nair, P. Blake, A. N. Grigorenko, K. S. Novoselov, T. J. Booth, T. Stauber, N. M. R. Peres, and A. K. Geim, *Science* **320**, 1308 (2008).

[23] A. B. Kuzmenko, E. van Heumen, F. Carbone, and D. van der Marel, *Phys. Rev. Lett.* **100**, 117401 (2008).

[24] G. Y. Guo, K. C. Chu, D. S. Wang, and C. G. Duan, *Phys. Rev. B* **69**, 205416 (2004).

[25] A. G. Marinopoulos, L. Reining, A. Rubio, and V. Olevano, *Phys. Rev. B* **69**, 245419 (2004).

[26] A. B. Djurišić and E. H. Li, *J. of Appl. Phys.* **85**, 7404 (1999).

[27] E. M. Lifshitz and L. P. Pitaevskii, "Statistical Physics Part 2," p.346, Butterworth-Heinemann, Oxford (2002).

[28] W. Z. Yang and J. P. Huang, *J. Appl. Phys.* **101**, 064903 (2007).

[29] V. Adrian Parsegian, "Van der Waals Forces," p.268, Cambridge University Press, New York, 2006.

[30] M. S. Tomaš, *Phys. Rev. A* **66**, 052103 (2002).

[31] S. Basu and D. Chakravorty, *Journal of Non-Crystalline Solids*, **352**, 380 (2006).

[32] P. Sheng and M. Gadenne, *J. Phys: Condens. Matter* **4**, 9735 (1992).

[33] L. N'eel, *Ann. Geophys.* (C.N.R.S.) **5**, 99 (1949).

[34] G. Xiao, S. H. Liou, A. Levy, J. N. Taylor, and C. L. Chien, *Phys. Rev. B* **34**, 7573 (1986).

[35] S. H. Masunaga, R. F. Jardim, P. F. P. Fichtner, J. Rivas, *Phys. Rev. B* **80**, 184428 (2009).

[36] J. F. Dobson, A. White, and A. Rubio, *Phys. Rev. Lett* **96**, 073201 (2006).

[37] G. G'omez-Santos, *Phys. Rev. B* **80**, 245424 (2009).

[38] L. A. Falkovsky and A. A. Varlamov, *Eur. Phys. J. B* **56**, 281 (2007).

[39] I. V. Fialkovsky, V. N. Marachevsky, and D. V. Vassilevich, *Phys. Rev. B* **84**, 035446 (2011).

[40] D. R. Smith, Willie J. Padilla, D. C. Vier, S. C. Nemat-Nasser and S. Schultz, *Phys. Rev. Lett.* **84**, 4184 (2000).

[41] C. G. Parazzoli, R. B. Greegor, K. Li, B. E. C. Koltenbah and M. Tanielian, *Phys. Rev. Lett.* **90**, 107401 (2003).

[42] G. Dolling, M. Wegener, C. M. Soukoulis, and S. Linden, *Opt. Letters* **32**, 53 (2007).

[43] H. J. Lezec, J. A. Dionne, and H. A. Atwater, *Science* **316**, 430 (2007).

[44] G. Goussetis, A. P. Feresidis and A. R. Harvey, *J. Mod. Opt.* **57**, 1 (2010).

[45] W. Cai, U. K. Chettiar, H.K. Yuan , V. C. de Silva, A. V. Kildishev, V. P. Drachev, and V .M. Shalaev, *Opt. Express* **15**, 3333 (2007).

[46] H. Yuan, U. K. Chettiar, W. Cai, A. V. Kildishev, A. Boltasseva, V. P. Drachev, and V. M. Shalaev, *Opt. Express* **15**, 1076 (2007)

[47] A. N. Grigorenko, A. K. Geim, H. F. Gleeson, Y. Zhang, A. A. Firsov, I. Y. Khrushchev and J. Petrovic, *Nature* **438**, 335 (2005).

[48] V. M. Shalaev, *Nat. Photonics* **1**, 41 (2007).

[49] J. Sarabadani, A. Naji, R. Asgari, and R. Podgornik, arXiv:1105.4241v1 (2011).